Geophysical Research Letters

RESEARCH LETTER
10.1029/2023GL107622

Moisture Sources and Pathways of Annual Maximum Precipitation in the Lancang-Mekong River Basin

Shuyu Zhang[1], Gengxi Zhang[2], Guoqing Gong[1], Thian Yew Gan[3], Deliang Chen[4], and Junguo Liu[1,5]

[1]School of Environmental Science and Engineering, Southern University of Science and Technology, Shenzhen, China, [2]College of Hydraulic Science and Engineering, Yangzhou University, Yangzhou, China, [3]Department of Civil and Environmental Engineering, University of Alberta, Edmonton, AB, Canada, [4]Department of Earth Sciences, University of Gothenburg, Gothenburg, Sweden, [5]Henan Provincial Key Laboratory of Hydrosphere and Watershed Water Security, North China University of Water Resources and Electric Power, Zhengzhou, China

Abstract Recent extremely heavy precipitation has led to substantial economic losses and affected millions of residences in the Lancang-Mekong River Basin (LMRB). This study analyzed the spatial-temporal characteristics of the annual maximum precipitation (R1X) of the LMRB and identified the moisture sources and pathways conducive to R1Xs using a Lagrangian back trajectory model. Results show that India Ocean and Bay of Bengal (IO/BOB), local evapotranspiration, and West Pacific Ocean and East China (WP/EC) are the three main moisture transport pathways of the R1Xs in LMRB, contributing 68.3%, 20.4% and 11.3% of the trajectories, respectively. R1Xs in the downstream eastern area are affected by tropical cyclones bringing large amounts of moisture from the WP/EC. As tropical cyclones shifted northward under climate change impact, more extreme precipitation occurred over the LMRB due to moisture coming from WP/EC, but those from the IO/BOB had decreased because of the slowdown of flows across the Equator.

Plain Language Summary Recent extremely heavy precipitation has led to more frequent floods, storm surges, and other natural hazards in the Lancang-Mekong River Basin, resulting in substantial economic losses and affecting millions of residences. This study used annual maximum precipitation to represent the extreme precipitation and analyzed its spatial-temporal characteristics and the moisture sources and pathways. Results show that the extreme precipitation of the upstream region mainly occurred in July, while that of the downstream region mainly occurred in August-September. The moisture pathways of the historical extreme precipitation were identified using a physical-based model, and are classified into three clusters using a machine-learning model. West Pacific Ocean and East China, local evapotranspiration, and Indian Ocean and Bay of Bengal (IO/BOB) are the three moisture transport pathways with contributions of 68.3%, 20.4%, and 11.3% to the total pathways. The tropical cyclones bring large amounts of moisture and mainly affect R1Xs in the downstream eastern area. Tropical cyclones shifted northward under climate change impact, and more extreme precipitation occurred over the LMRB due to moisture coming from the West Pacific Ocean and East China, but those from the IO and BOB had decreased because of the slowdown of flows across the Equator.

Key Points:

- The timing of the annual maximum precipitation of the Lancang-Mekong River Basin (LMRB) varies from July to September
- The extreme precipitation of the LMRB mainly received moisture from the Indian Ocean to the West Pacific Ocean
- Tropical cyclones will bring more extreme precipitation to the LMRB under climate change

Supporting Information:

Supporting Information may be found in the online version of this article.

Correspondence to:

J. Liu,
junguo.liu@gmail.com

Citation:

Zhang, S., Zhang, G., Gong, G., Gan, T. Y., Chen, D., & Liu, J. (2024). Moisture sources and pathways of annual maximum precipitation in the Lancang-Mekong River Basin. *Geophysical Research Letters*, *51*, e2023GL107622. https://doi.org/10.1029/2023GL107622

Received 4 DEC 2023
Accepted 4 MAR 2024

Author Contributions:

Conceptualization: Shuyu Zhang
Funding acquisition: Gengxi Zhang, Junguo Liu
Methodology: Shuyu Zhang, Gengxi Zhang
Project administration: Junguo Liu
Software: Shuyu Zhang, Gengxi Zhang
Supervision: Thian Yew Gan
Validation: Shuyu Zhang
Writing – original draft: Shuyu Zhang, Guoqing Gong

1. Introduction

Recent occurrences of more frequent and intensive extreme precipitation (Irannezhad et al., 2021; Lemus-Canovas, 2022; C. Li et al., 2019; J. Li et al., 2021; S. Wang et al., 2021; Zhao et al., 2023) have resulted in multiple natural hazards such as floods, landslides, and major urban inundation. The population exposed to hazards caused by extreme precipitation is projected to increase with continuous global warming (Gudmundsson et al., 2021; X. Li et al., 2022; Smith et al., 2019; Swain et al., 2020). As one of the most important transboundary river basins, the Lancang-Mekong River Basin (LMRB) comprises a complex geographical distribution of land, ocean, and terrains, a high agriculture and industry-based economy, and a high human density, rendering it highly vulnerable to impacts of hazards resulted from worsening extreme precipitation under the effects of global warming, often with disastrous consequences (Ge et al., 2019, 2021; Irannezhad et al., 2021; Shaw et al., 2022; Y. Wang et al., 2023).

Under significant warming, atmospheric water vapor content has increased leading to more precipitation (Ge et al., 2019). Theoretically, the global mean precipitation will increase by 7% per °C rise in air temperature (B. Liu et al., 2020). However, for the development of extreme precipitation, abnormal atmospheric moisture transport is

Writing – review & editing: Shuyu Zhang, Gengxi Zhang, Thian Yew Gan, Deliang Chen

essential (Allan et al., 2020; Gimeno et al., 2016; B. Liu et al., 2020; Nie & Sun, 2022), which has been the focus of many recent studies on extreme precipitation events. For instance, the record-breaking precipitation in Henan, China, in July 2021, leading to 398 deaths and more than 20 billion dollars in damage, was due to the combined effects of a sustained western Pacific subtropical high and a strong moisture input from tropical cyclone In-Fa and Cempaka (Ma et al., 2022; Nie & Sun, 2022; S. Zhang et al., 2022). In August 2022, the extreme precipitation in Pakistan that displaced 33 million of residents was mainly caused by the significant moisture influx from two atmospheric rivers from the Arabian Sea (Nanditha et al., 2023).

Many current studies mainly focus on the moisture transport mechanism of individual extreme events or the temporal changes in precipitation (Sun et al., 2021). However, the long-term characteristics of the moisture transport mechanism associated with extreme precipitation are still not well understood, which is crucial to regional flood control, reservoir regulation, and risk management (Tan, Gan, & Chen, 2018). LMRB is located in the "cross-region" between two monsoon systems: the Indian Summer Monsoon (ISM) and the East Asian summer monsoon, whose covariance was found to modulate the interannual variability of precipitation of LMRB (Chen et al., 2019; R. Yang et al., 2019). LMRB also suffers from tropical cyclones, frequently, and tropical cyclone-induced rainfall is the main surface water resource in specific months of the east region (Chhin et al., 2016; Takahashi & Yasunari, 2008). As for extreme precipitation, analyzing the moisture transport pathways associated with historical extreme precipitation may improve the understanding of the mechanisms behind the recent changes in the frequency and intensity of extreme precipitation.

This study uses a Lagrangian trajectory model to simulate the moisture transport process associated with the annual maximum precipitation of LMRB over 1959–2021. Lagrangian trajectory model could provide moisture transport trajectories from evaporation to precipitation (Stein et al., 2015) and has been widely used in the moisture transport analysis associated with extreme events (Nie & Sun, 2022; C. Zhang et al., 2019). The simulated moisture transport trajectories were clustered through an unsupervised machine learning method to identify the main moisture transport patterns associated with the annual maximum precipitation over LMRB. The background of atmospheric circulations corresponding to different moisture transport patterns was further analyzed to reveal mechanisms behind the variations of extreme precipitation regulated by different moisture transport patterns.

2. Materials and Methodology

2.1. Precipitation Data and Definition of Extreme Precipitation

In this study, the daily precipitation data from the European Center for Medium-range Weather Forecasts Reanalysis version 5 (ERA-5) was used (Hersbach et al., 2020), which has 1158 grids within LMRB. ERA-5 is a widely-used reanalysis data set with high resolution (0.25°) and long duration (1959 to present) (Yatagai & Zhao, 2014), with a consistent performance in describing the spatial-temporal variations of precipitation worldwide well recognized in recent studies (Deng et al., 2020; Nogueira, 2020; Xu et al., 2020). The annual maximum daily precipitation (R1X) with its corresponding timing, in Julian days, for each grid within LMRB over 1959–2021 was extracted to represent the extreme precipitation. Over 60,000 historical extreme precipitation events in LMRB were compiled and analyzed for their moisture transport process. To analyze the atmospheric background of the moisture transport associated with the R1X in LMRB, the wind fields, geopotential height (GPH), and sea surface temperature (SST) were also extracted from the NCEP/NCAR-R1 data set (Kalnay et al., 1996), which has been widely used in the analysis of anomalous atmospheric circulation associated with extreme events (Tan, Gan, Chen, et al., 2018; S. Zhang et al., 2022).

2.2. Backward Trajectories Identified by HYSPLIT Model

The Hybrid Single-Particle Lagrangian Integrated Trajectory (HYSPLIT) model version 5.0.0, developed by the Air Resources Laboratory of the National Oceanic and Atmospheric Administration, was used to track moisture sources and pathways for each extreme precipitation event (Draxler & Hess, 1998; Stein et al., 2015). HYSPLIT is one of the most commonly used models for back-trajectory analysis in identifying the sources of air masses and source-receptor relationships. The application of HYSPLIT is expanded from tracking air pollutants trajectories at the beginning to the analysis of anomalous moisture transport associated with extreme weather (Guan et al., 2022). HYSPLIT could generate the three-dimensional pathway for an air parcel that arrives at a given location at an arbitrary location and time. The six-hourly temperature, GPH, air temperature, three-dimensional

wind fields, and relative humidity data at multiple pressure levels from the National Centers for Environmental Prediction-National Center for Atmospheric Research Reanalysis 1 (NCEP/NCAR-R1) (Kalnay et al., 1996), were used to drive the HYSPLIT model. In this study, we calculated the hourly locations of air parcels for 8 days before the extreme precipitation event, for the moisture retained in the atmosphere for about 8 days (Trenberth, 1998), which should be sufficient to identify most moisture sources. For each R1X, four arriving times at 0 heights were set, and then four trajectories were obtained for each extreme precipitation. In this study, more than 300,000 trajectories were compiled through the R package "splitr" (Cohen et al., 2015; Draxler, 1999; Draxler & Hess, 1998), and those trajectories with a loss in specific humidity were taken as the moisture origin.

2.3. Trajectory Clusters

To refine information from numerous trajectories, trajectories clustering analysis was applied to extract moisture transport patterns (Gustafsson et al., 2010), and the Self-Organizing Map (SOM) was used in this study to cluster the identified trajectories into three groups. As an unsupervised artificial neural network, SOM could group similar records and re-organize them into arrays that could compose a map of the pattern space without any prior information about the group to reduce the dimensions of the data space (Kohonen, 1990). Details of SOM which has been widely used in clustering climate data about the algorithm and its application in climate data can be found in Cassano et al. (2015), Higgins and Cassano (2009), Tan, Gan, and Chen (2018), Yu et al. (2018). This study used the R package "kohonen" to conduct the unsupervised SOMs (Wehrens & Buydens, 2007; Wehrens & Kruisselbrink, 2018). The quality of classification in SOM is primarily assessed using the Quantization Error, which is also calculated through the R "kohonen" package. Quantization errors indicate the magnitude of the intra-cluster error for each neuron, and a lower value indicates higher SOM typing quality. In this study, each trajectory group represents a moisture transport pattern that dominates the pathways transferring water vapor leading to extreme precipitation events in each grid. For each trajectory group, the temporal and spatial changes of each trajectory pattern could be estimated, as well as the frequency and its contribution to the regional average extreme precipitation. In addition, the corresponding atmospheric circulation background of the three kinds of trajectory patterns was extracted and further analyzed.

3. Results

3.1. Spatial-Temporal Characteristics of the Annual Maximum Precipitation Over the LMRB

The spatial distribution of the timing (in Julian days) and the magnitudes of the multi-year average R1Xs were presented in Figure 1. It is found that the spatial variation of the multi-year average R1Xs could be as large as 100 mm, that the eastern edge of the middle reach of LMRB could be higher than 100 mm, while the source region of the Lancang River that located within the Tibet Plateau is only about 10 mm (Figure 1b). In the downstream of LMRB, R1X is generally higher in the east than in the west, and higher in the north than in the south. For instance, Laos has R1X of about 60–70 mm while Cambodia and southern Thailand just have nearly 20–30 mm because Laos has more mountainous terrain (Figure 1b). In terms of the timing, R1Xs over the LMRB mainly occur from late June to September with a range of about 100 days. R1Xs in the upstream tend to occur early but mainly in July. The mountainous region in Laos also has R1Xs in July but the plateau region within Thailand at a similar latitude generally has R1Xs occurring in August. The R1Xs in downstream of LMRB generally occur in August, except in west Cambodia. Close to the Gulf of Thailand, west Cambodia often has the latest R1Xs occurring in September (Figure 1c). The large variations within the spatial distribution of timing and magnitude of the R1Xs should be the combined results of different moisture transport mechanisms and terrains.

3.2. Moisture Sources and Pathways for R1X

The moisture sources and pathways associated with the R1X over LMRB during 1959–2021 were analyzed and clustered into three groups using the HYSPLIT model and SOM, respectively. Figure 2 shows the total and clustered trajectories. It shows that R1Xs mainly receive moisture from the Indian Ocean (IO), the West Pacific Ocean (WP), and the mainland of Eurasia continent (Figure 2a). According to the clustering results of SOM, moisture from the IO travels through the Bay of Bengal (IO/BOB) to the LMRB, which as the main moisture transport pathway, contributed 68.33% of the total trajectories associated with R1Xs (Figure 2b1). The second clusters of trajectories include the moisture transport pathways from local terrains and neighboring sea surface and inland Eurasia (hereby abbreviated as Local), which accounts for 20.41% of the total trajectories (Figure 2c1).

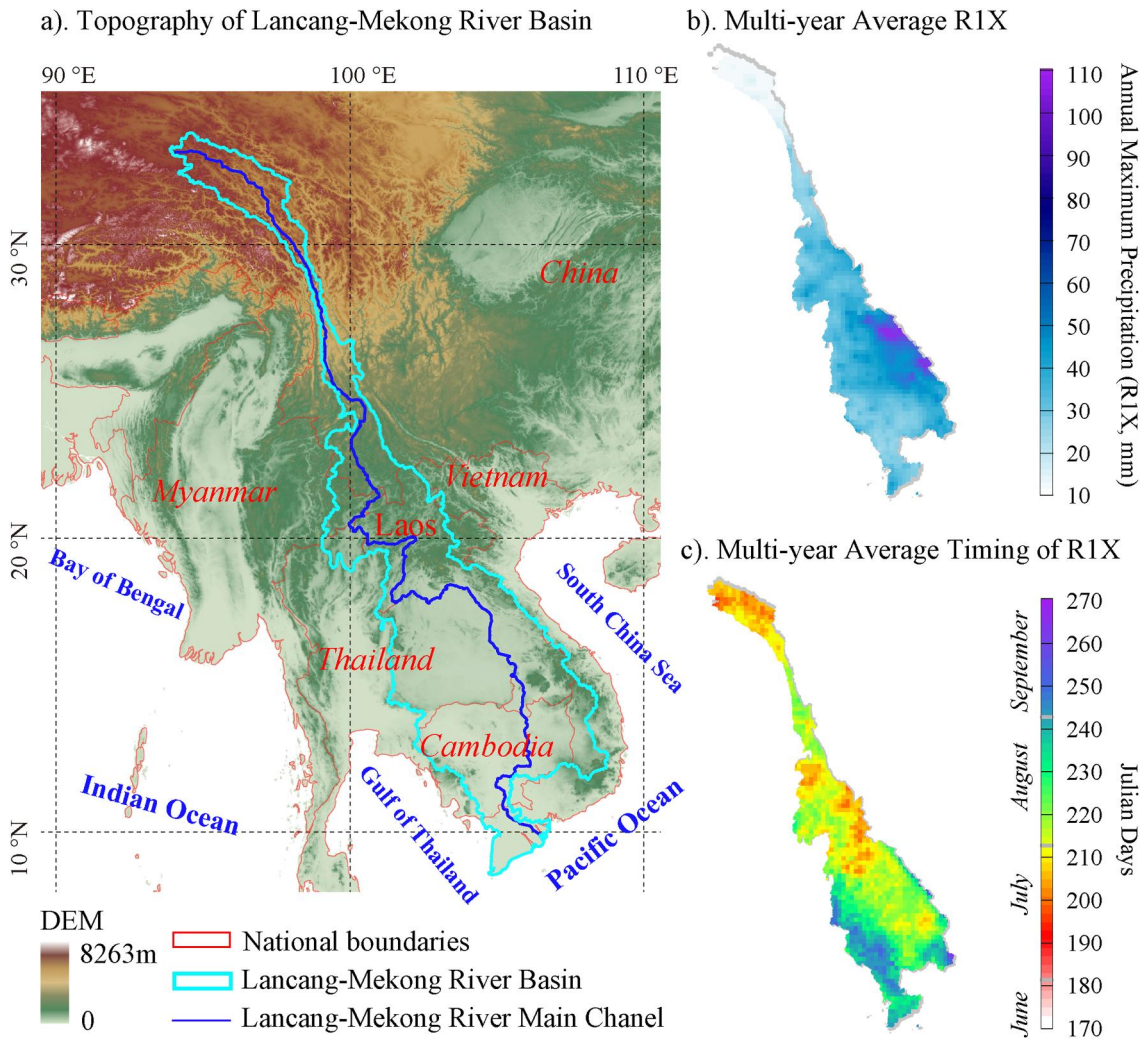

Figure 1. The topography of the Lancang-Mekong River Basin and the multi-year average annual maximum daily precipitation magnitude (b) and the timing (in Julian Days) (c) over 1959–2021.

The third cluster contains moisture pathways from the Northwest Pacific Ocean and East China (WP/EC) that constitute 11.26% of the total trajectories (Figure 2d1). Therefore, moisture from IO/BOB contributes most trajectories to the R1Xs of the LMRB.

Based on the statistical analysis of grids that receive moisture from the three clustered moisture transport pathways, it is found that the main moisture-contributing pathways are quite different among regions. The spatial distributions of R1Xs associated with three types of moisture transport patterns are also presented. R1Xs over most of the downstream of LMRB, especially the southwestern LMRB, receive moisture from the IO/BOB, where the contributions from IO/BOB exceed 75% (Figure 3b2). The second cluster of pathways that transport moisture from the local and neighboring sea and inland Eurasia continents mainly contribute to the R1Xs of the upstream of LMRB, with more than 75% of total trajectories (Figure 3c2). It also influences R1Xs over the middle-stream region of LMRB where its contribution is less. The pathways from the WP/EC mainly contribute to the R1Xs over the east region of the middle-stream region more than other places but with a lower percentage of trajectories compared with the other two pathways (Figure 3d2).

3.3. Temporal Changes in Moisture Transport Pathways

After estimating trajectories of air parcels and their patterns associated with the R1Xs over LMRB, we then analyzed the temporal changes of the three patterns from 1959 to 2021 (Figure 3). Results obtained from the linear

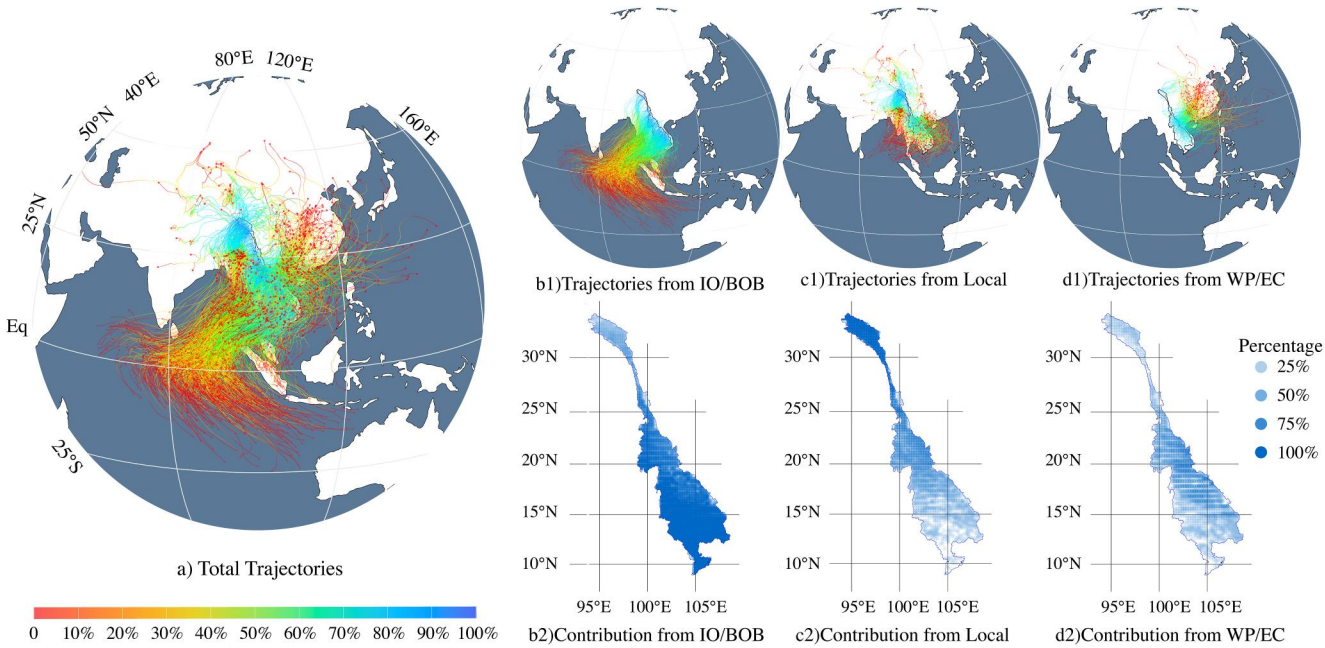

Figure 2. Total (a) and clustered ((b1) for Indian Ocean/Bay of Bengal, (c1) for Local evapotranspiration, and (d1) for West Pacific/East China) trajectories of air parcels reaching Lancang-Mekong River Basins during the annual maximum precipitation of 1959–2021. The contribution of moisture is presented by colors. Spatial distribution of the percentage of trajectories from three clusters (b2, c2, and d2).

regression of the contributions from the three moisture transport patterns are quite different. The IO/BOB pattern shows a decreasing trend with a statistical significance in the contribution to the total trajectories, which occasionally exceeded 80% before 1980 but decreased to less than 50% in some years after 1990 (Figure 3a). The second pattern originated from the local and nearby sea surface and inland Eurasia does not have any monotonic trend in the contribution with an average between 20% and 25% (Figure 3b). The WP/EC pattern that originates from Northwest Pacific Ocean and East China shows an increasing trend that is statistically significant although the contribution is much smaller than other two patterns (Figure 3c).

Figure 4 shows probabilistic density functions of moisture sources from IO/BOB and WP/EC patterns concerning the locations (latitude and longitude) for each decade. Moisture sources of IO/BOB are mainly located within the region between 70°E–110°E and 20°S–10°N, with more than 60% located in 80°E–100°E and 10°S–5°N and the general northwestern direction of the moisture sources was also demonstrated (Figures 4a1 and 4a2). Sources of the WP/EC pattern were more concentrated between 100°E–130°E and 20°N–40°N (Figures 4c1 and 4c2), but

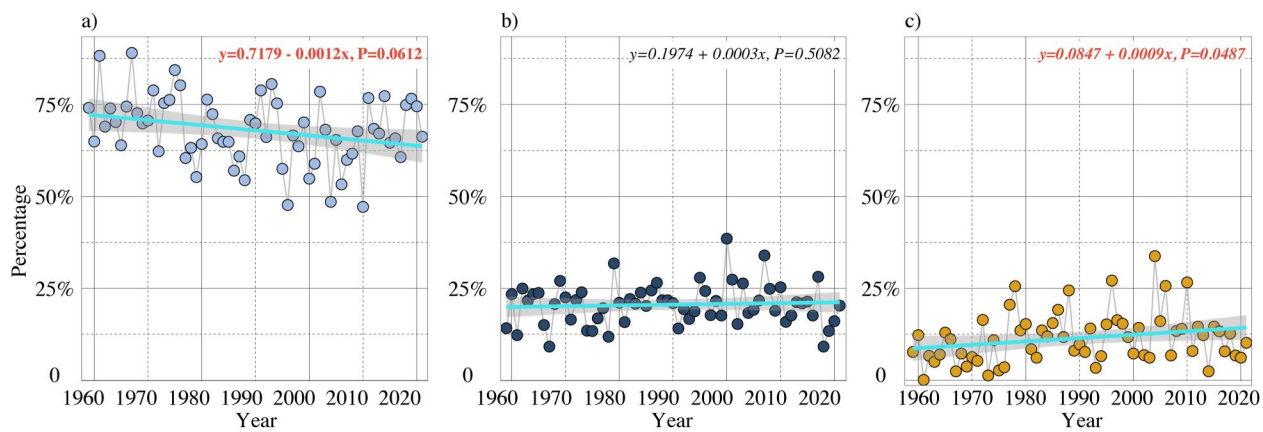

Figure 3. The temporal changes of contribution to total trajectories of three moisture transport patterns. (b) for Indian Ocean/Bay of Bengal, (c) for Local evapotranspiration, and (d) for West Pacific/East China.

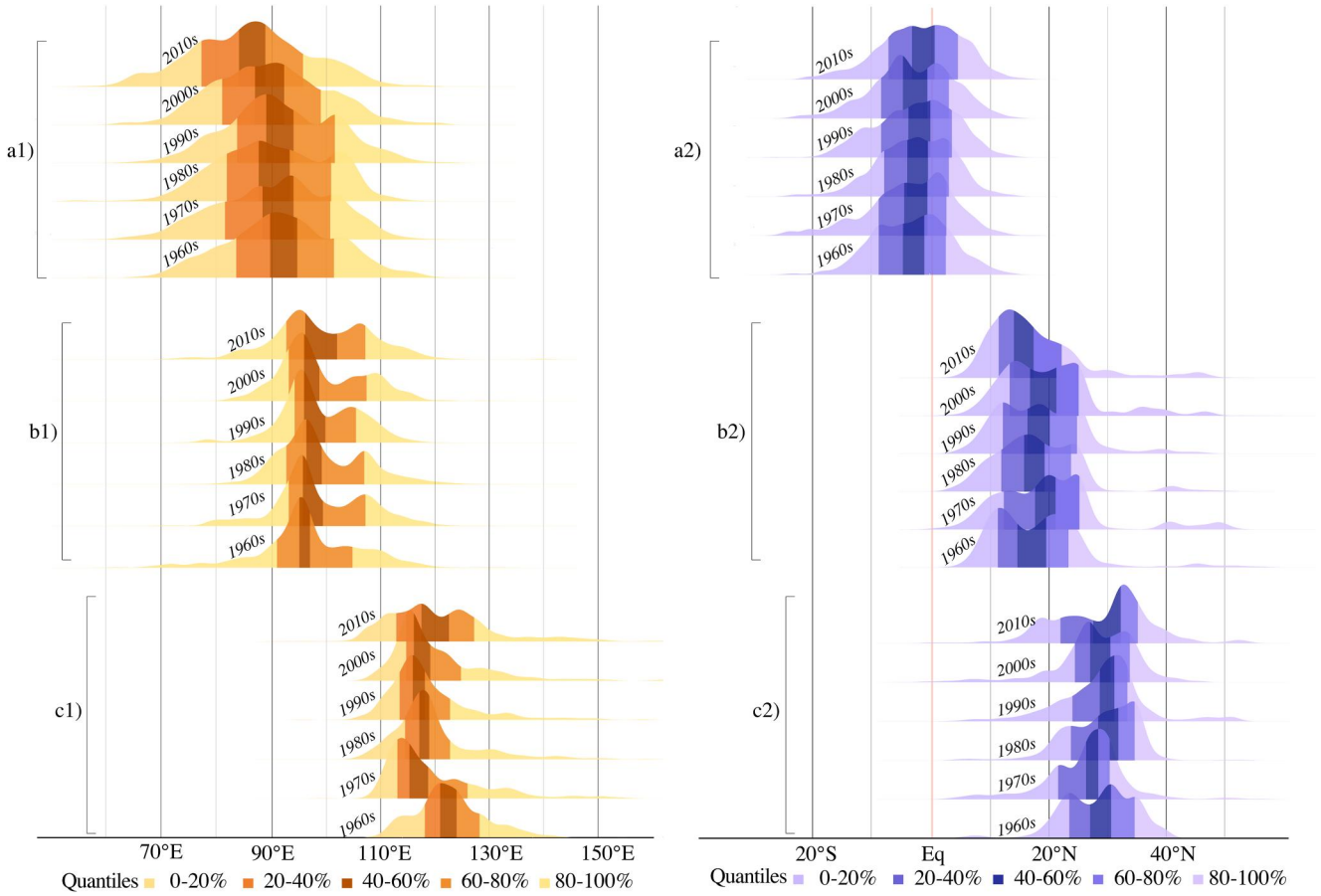

Figure 4. The decadal variation of the location (*1 for longitude, and *2 for latitude) of the moisture sources of three patterns: a* for Indian Ocean/Bay of Bengal, b* for Local evapotranspiration, and c* for West Pacific/East China.

they swung in different directions within a range instead of moving toward one direction only. About 60% of the moisture sources were located at 115°E–120°E in the 1960s swung westward to 95°E–150°E in the 1970s, and moved eastward to 110°E–115°E in the 2010s (Figure 4c1). Along with the movement of moisture sources, the range of the longitudes involved also expanded from 105°E–130°E to 100°E–140°E. In the zonal direction, there was a minor northward movement (Figure 4c2). Compared with IO/BOB and WP/EC patterns, the LOCAL is more consistent at both the range and the center region of moisture sources. The movement of the moisture sources may reflect the changes in moisture transport mechanisms.

3.4. Atmospheric Circulation of Moisture Transport

To further examine the atmospheric background of different moisture transport patterns, we also analyzed the GPH at 500mb, the SST, and wind fields (Uwind and Vwind) associated with the moisture transport patterns (Figure 5). For the IO/BOB pattern, the Northern Hemisphere were anomalously warm, especially North Pacific Ocean and the Arctic Ocean, but the southern Hemisphere was cold, particularly the circumpolar sea surface over 60°S, and the GPH over Siberia and Northwest Pacific Ocean was high (Figure 5a1). There was also a strong westerly wind under the IO/BOB pattern, which consists of cross-equatorial flows (CEF) at 45° N, known as Somali Jet, and the CEF at 85°N, both of which were driven by the Coriolis Force and regulated by the terrains (Figure 5a2). Given the IO/BOB pattern contributes more than 64% of the moisture trajectories associated with R1Xs of LMRB, it seems that these strong low-level jets are mainly responsible for the extreme precipitation of LMRB. When the Local Pattern dominates the R1Xs, a strong northeasterly wind from the South China Sea and a southwesterly wind from the BOB "collided" over the LMRB, which resulted in heavy precipitation (Figure 5b2) and the Northwest Pacific Ocean was anomalously warm (Figure 5b1). Under the WP/EC pattern, two noticeable cyclones were formed over the South China Sea and the far-reached

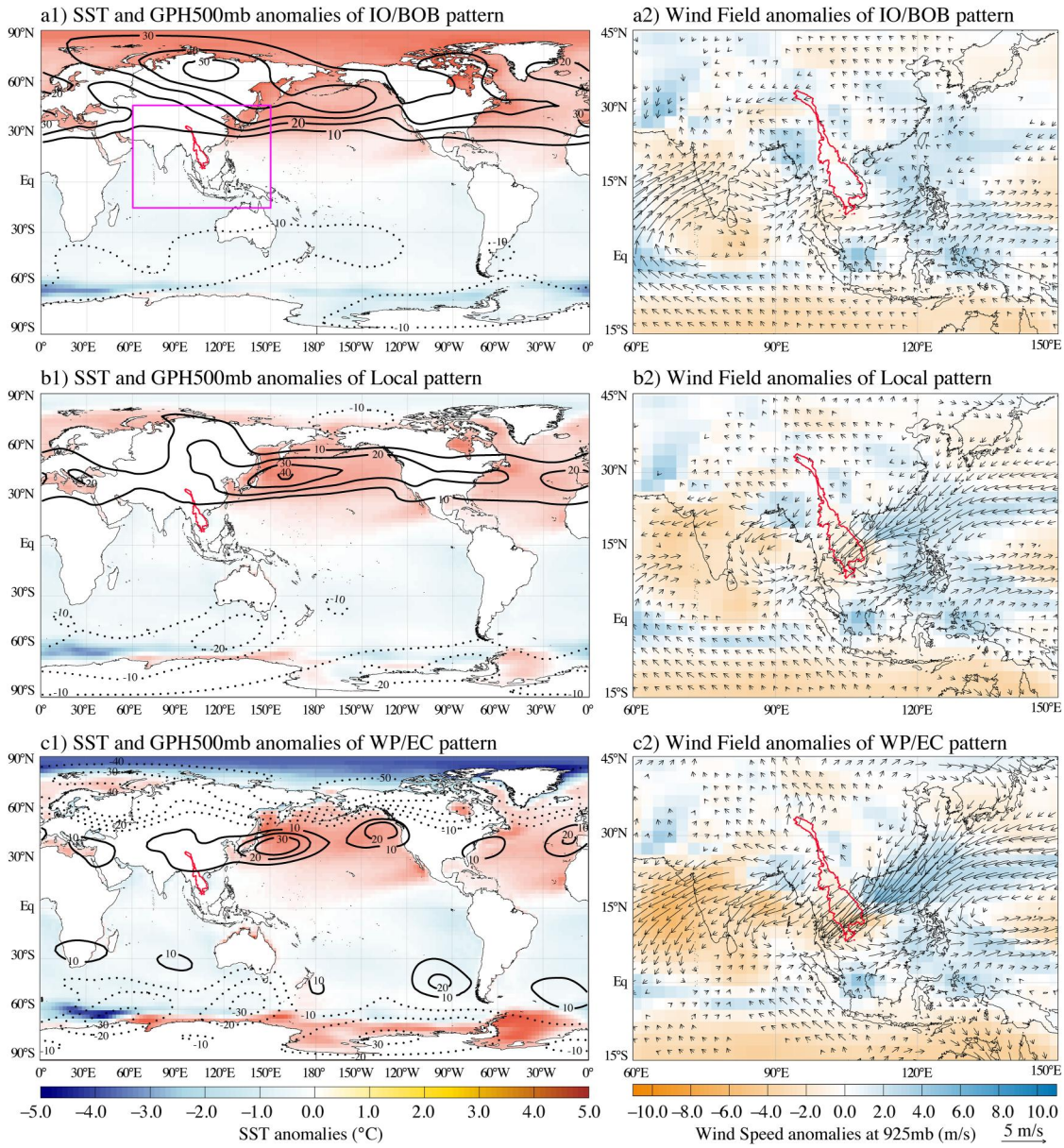

Figure 5. Atmospheric circulation background of the three moisture transport patterns (a* for Indian Ocean/Bay of Bengal, b* for Local evapotranspiration, and c* for West Pacific/East China) associated with the annual maximum precipitation over the Lancang-Mekong River basin. 1* shows Geopotential height at 500mb (contours) and the sea surface temperature (shaded) anomalies. 2* shows the wind speed anomalies (shaded) and wind direction (arrows).

West Pacific Ocean which facilitated the strong moisture transport from the Northwest Pacific Ocean, crossing the downstream of LMRB and even reaching the Indian Peninsula (Figure 5c2). The Arctic Ocean was noticed to be colder than the climatology (multi-year average over 1959–2022), and the Mascarene High is also weaker, which is the origin of the ISM and the Somali Jet (Figure 5c1). The North Pacific was found to have two warm pools (Figure 5c1). Which should be conducive to the formation of tropical cyclones. Therefore, it could be concluded that the CEF and the northeasterlies generated by tropical cyclones dominate the R1Xs. The CEF brings relatively mild R1Xs but it affects a large area in the middle and downstream of LMRB, while the very strong R1Xs in the west of mid-LMRB, were usually brought by tropical cyclones. According to the sixth Annual Report of IPCC, tropical cyclones show an increasing trend with the exacerbating climate change, as well as the intensity and frequency of extreme precipitation they bring (Douville et al., 2021), which is consistent with the results of this study.

4. Discussion of Results

Moisture transport patterns associated with the R1Xs of LMRB are investigated. Temporal changes in the contributions from different moisture transport patterns could indicate future trends of extreme precipitation. The possible approaches of climate change and human activities affecting the extreme precipitations over LMRB will be further discussed.

As R1Xs were chosen to represent the extreme precipitation, the number of simulated trajectories is constant for each year, equal to the total number of grids, and the contribution of each pattern should be consistent with the area affected by the pattern. The contribution from the West Pacific/East China (WP/EC) pattern shows an increasing trend (Figure 3c) at the expense of decreasing contributions from the IO/BOB pattern (Figure 3a). Therefore, the WP/EC pattern is responsible for the R1Xs of a gradually larger area. According to Figure 5c2, the anomalous northeasterly wind generated by cyclones in the Western North Pacific would lead to the formation of extreme precipitation. These results support recent findings of the northward shift of landfall locations of Western North Pacific tropical cyclones and the observed increasing frequency of tropical cyclones occurring in the West Pacific Ocean (Basconcillo & Moon, 2022; K. S. Liu & Chan, 2022; Tran et al., 2022; Yamaguchi et al., 2020). As tropical cyclones bring a larger volume of precipitation and later occurrences of R1Xs than the monsoon, there will be a larger area exposed to extreme precipitation and following natural hazards, like flooding, landslides, and debris flow. Moreover, local water resource management will also face a large challenge. It is essential to reliably predict the magnitude of such hazards and to develop mitigation measures against hazards using structural and non-structural solutions. However, whether the IO/BOB pattern is bringing decreasing precipitation to the LMRB needs further discussion. The cross-equatorial flow and low-level Somali Jet that brings very humid water vapor to LMRB (Figure 5a2) is further analyzed. The wind field associated with moisture sources of the IO/BOB moisture transport pattern (85°E–95°E, 5°N–25°N) was extracted and plotted in Figure S1. Significant decreasing trends were found in both the meridional and the zonal wind speed, which will inevitably result in the decline of moisture transport. It provides evidence to support past findings that reduced evaporation from the regional moisture sources was attributed to the decline of moisture transport from the cross-equatorial flow and Somali Low-level Jets (Bajrang et al., 2023). These changes could be related to the variations of the ISM (B. B. Goswami et al., 2010), which has weakened under the impact of global warming (Schewe & Levermann, 2012) and is likely responsible for the decline of summer rainfall over large parts of South Asia over the past five to six decades (Bollasina et al., 2011; B. N. Goswami et al., 2006; Sinha et al., 2015). However, some studies show the revival of ISM in recent decades should be related to its multi-decadal variability (Bajrang et al., 2023; Jin & Wang, 2017), which was found to have a relationship with the IO Dipole (Cai et al., 2014; Ratna et al., 2021; C. Wang & Wang, 2019). East Asia Summer Monsoon and the El Nino events were also found to have a significant relationship with the variation of CEF through SST (Hu et al., 2018; Wilson et al., 2018). However, this relationship is also changing with the global climate change and is still under discussion. Moreover, the unique topography of the Tibetan Plateau also influences moisture transport patterns, especially under the impact of significant warming. The strong local upward convection, along with the surface radiative heating, would facilitate the water vapor confluence and suction dynamic effects (Cheng et al., 2022; X. Li et al., 2022; Y. Wang et al., 2023; Xu et al., 2019; K. Yang et al., 2010).

Additionally, rapid urbanization (Falga & Wang, 2022; Singh et al., 2019), melting of snow cover (Bamzai & Shukla, 1999), cooling effects of aerosols (Bollasina et al., 2011; Sinha et al., 2015), and rising concentrations of greenhouse gases (Cai et al., 2014; Sinha et al., 2015) could affect the formation of extreme precipitation due to less convective available potential energy higher convective inhibition energy and stronger atmospheric stability (Bajrang et al., 2023; Muller & Takayabu, 2020; Ramanathan et al., 2005). However, the influence of human activities on extreme precipitation of LMRB is still under considerable debate, which will be studied to better understand the mechanisms of the moisture transport over LMRB.

5. Summary and Conclusions

In this study, the moisture sources and transport pathways conducive to the annual maximum daily precipitation (R1Xs) over the LMRB from 1959 to 2021 were analyzed. The R1X of the upstream region primarily occurred in July, while that of the downstream region mainly occurred from August to September. Spatially, the lower region of LMRB experienced higher and later occurrences of R1Xs than the upper region, while the eastern region experienced higher and later occurrences of R1Xs than the western region. By using a Lagrangian back trajectory

model and the Self-Organize Map (SOM) method, three main moisture transport pathways were identified over LMRB. The IO/BOB, local evapotranspiration, and West Pacific/East China (WP/EC) are the three main moisture sources, contributing to 68.3%, 20.4%, and 11.3% to the total trajectories, respectively. Different moisture transport patterns contribute to the R1Xs in different regions under different atmospheric circulation backgrounds. For the upper region of LMRB, evapotranspiration from the local and neighboring terrestrial and oceanic surfaces provides the main moisture sources. The moisture from the IO/BOB transported through the cross-equator flow mainly contributes to most lower regions of LMRB, under the strong influence of the ISM. For the eastern and lower regions of LMRB, R1Xs are the highest and mainly attributed to tropical cyclones bringing large amounts of moisture from the WP/EC to LMRB. As tropical cyclones shifted northward under the influence of climate warming, more extreme precipitation over the LMRB will be fed by the moisture from WP/EC, while those from the IO/BOB will decrease with the slowdown of cross-tropical flows partly due to the oscillation of the ISM. As LMRB has a large population and currently undergoes rapid urbanization, it will be essential for us to understand the moisture transport mechanisms associated with extreme precipitation over LMRB, to increase our predictive skill on future flood hazards, and to develop effective mitigation measures against such hazards expected to be a growing threat under the impact of climate change.

Conflict of Interest

The authors declare no conflicts of interest relevant to this study.

Data Availability Statement

ERA-5 reanalysis data (Hersbach et al., 2020), NCEP/NCAR reanalysis data (Kalnay et al., 1996), and open-source R packages "splitr" (Cohen et al., 2015; Draxler, 1999; Draxler & Hess, 1998) and "kohonen" (Wehrens & Buydens, 2007; Wehrens & Kruisselbrink, 2018) helped us immensely. The datasets and codes are available from the repository in the corresponding in-text citation.

Acknowledgments
The National Natural Science Foundation of China funded this study by Grant 42361144001. The Shenzhen Science and Technology Innovation Program with Grant K21296405 and the Natural Science Foundation of Jiangsu Province with Grant BK20220590 are also acknowledged for partially financing this study. The author would like to thank the Henan Provincial Key Laboratory of Hydrosphere and Watershed Water Security, Strategic Priority Research Program of the Chinese Academy of Sciences, Grants: XDA20060401, XDA20060402. All authors discussed the results and contributed to the preparation of the manuscript.

References

Allan, R. P., Barlow, M., Byrne, M. P., Cherchi, A., Douville, H., Fowler, H. J., et al. (2020). Advances in understanding large-scale responses of the water cycle to climate change. *Annals of the New York Academy of Sciences*, *1472*(1), 49–75. https://doi.org/10.1111/nyas.14337

Bajrang, C., Attada, R., & Goswami, B. N. (2023). Possible factors for the recent changes in frequency of central Indian Summer Monsoon precipitation extremes during 2005–2020. *npj Climate and Atmospheric Science*, *6*(1), 120. https://doi.org/10.1038/s41612-023-00450-y

Bamzai, A. S., & Shukla, J. (1999). Relation between Eurasian snow cover, snow depth, and the Indian summer monsoon: An observational study. *Journal of Climate*, *12*(10), 3117–3132. https://doi.org/10.1175/1520-0442(1999)012<3117:rbescs>2.0.co;2

Basconcillo, J., & Moon, I.-J. (2022). Increasing activity of tropical cyclones in East Asia during the mature boreal autumn linked to long-term climate variability. *npj Climate and Atmospheric Science*, *5*(1), 4. https://doi.org/10.1038/s41612-021-00222-6

Bollasina, M. A., Ming, Y., & Ramaswamy, V. (2011). Anthropogenic aerosols and the weakening of the South Asian summer monsoon. *Science*, *334*(6055), 502–505. https://doi.org/10.1126/science.1204994

Cai, W., Santoso, A., Wang, G., Weller, E., Wu, L., Ashok, K., et al. (2014). Increased frequency of extreme Indian Ocean Dipole events due to greenhouse warming. *Nature*, *510*(7504), 254–258. https://doi.org/10.1038/nature13327

Cassano, E. N., Glisan, J. M., Cassano, J. J., Gutowski, W. J., & Seefeldt, M. W. (2015). Self-organizing map analysis of widespread temperature extremes in Alaska and Canada. *Climate Research*, *62*(3), 199–218. https://doi.org/10.3354/cr01274

Chen, A., Ho, C.-H., Chen, D., & Azorin-Molina, C. (2019). Tropical cyclone rainfall in the mekong River Basin for 1983–2016. *Atmospheric Research*, *226*, 66–75. https://doi.org/10.1016/j.atmosres.2019.04.012

Cheng, Q., Fan, G., & Zhu, L. (2022). Characteristics and changes in the atmospheric water cycle of the Tibetan Plateau vortex. *Theoretical and Applied Climatology*, *151*(3–4), 1601–1614. https://doi.org/10.1007/s00704-022-04273-4

Chhin, R., Trilaksono, N. J., & Hadi, T. W. (2016). Tropical cyclone rainfall structure affecting Indochina peninsula and lower mekong river basin (LMB). *Journal of Physics: Conference Series*, *739*, 012103. https://doi.org/10.1088/1742-6596/739/1/012103

Cohen, M. D., Stunder, B. J. B., Rolph, G. D., Draxler, R. R., Stein, A. F., & Ngan, F. (2015). NOAA's HYSPLIT atmospheric transport and dispersion modeling system [Software]. *Bulletin of the American Meteorological Society*, *96*(12), 2059–2077. https://doi.org/10.1175/bams-d-14-00110.1

Deng, K., Jiang, X., Hu, C., & Chen, D. (2020). More frequent summer heat waves in southwestern China linked to the recent declining of Arctic sea ice. *Environmental Research Letters*, *15*(7), 074011. https://doi.org/10.1088/1748-9326/ab8335

Douville, H., Raghavan, K., Renwick, J., Allan, R. P., Arias, P. A., Barlow, M., et al. (2021). Water cycle changes. In *Climate change 2021: The physical science basis. Contribution of working group I to the sixth assessment Report of the intergovernmental panel on climate change*. Cambridge University Press.

Draxler, R. R. (1999). HYSPLIT4 user's guide [Software]. *NOAA Air Resources Laboratory, Silver Spring, MD*. Retrieved from https://ww2.arb.ca.gov/sites/default/files/2020-10/HYSPLIT4%20USER%27s%20GUIDE.pdf

Draxler, R. R., & Hess, G. D. (1998). An overview of the HYSPLIT_4 modeling system of trajectories, dispersion, and deposition [Software]. *Australian Meteorological Magazine*, *47*, 295–308. Retrieved from https://www.researchgate.net/publication/239061109_An_overview_of_the_HYSPLIT_4_modelling_system_for_trajectories

Falga, R., & Wang, C. (2022). The rise of Indian summer monsoon precipitation extremes and its correlation with long-term changes of climate and anthropogenic factors. *Scientific Reports*, *12*(1), 11985. https://doi.org/10.1038/s41598-022-16240-0

Ge, F., Zhu, S., Luo, H., Zhi, X., & Wang, H. (2021). Future changes in precipitation extremes over southeast Asia: Insights from CMIP6 multi-model ensemble. *Environmental Research Letters*, *16*(2), 024013. https://doi.org/10.1088/1748-9326/abd7ad

Ge, F., Zhu, S., Peng, T., Zhao, Y., Sielmann, F., Fraedrich, K., et al. (2019). Risks of precipitation extremes over southeast Asia: Does 1.5°C or 2° C global warming make a difference? *Environmental Research Letters*, *14*(4), 044015. https://doi.org/10.1088/1748-9326/aaff7e

Gimeno, L., Dominguez, F., Nieto, R., Trigo, R., Drumond, A., Reason, C. J., et al. (2016). Major mechanisms of atmospheric moisture transport and their role in extreme precipitation events. *Annual Review of Environment and Resources*, *41*(1), 117–141. https://doi.org/10.1146/annurev-environ-110615-085558

Goswami, B. B., Mukhopadhyay, P., Mahanta, R., & Goswami, B. N. (2010). Multiscale interaction with topography and extreme rainfall events in the northeast Indian region. *Journal of Geophysical Research*, *115*(D12), D12114. https://doi.org/10.1029/2009jd012275

Goswami, B. N., Venugopal, V., Sengupta, D., Madhusoodanan, M. S., & Xavier, P. K. (2006). Increasing trend of extreme rain events over India in a warming environment. *Science*, *314*(5804), 1442–1445. https://doi.org/10.1126/science.1132027

Guan, Y., Gu, X., Slater, L. J., Li, L., Kong, D., Liu, J., et al. (2022). Tracing anomalies in moisture recycling and transport to two record-breaking droughts over the Mid-to-Lower Reaches of the Yangtze River. *Journal of Hydrology*, *609*, 127787. https://doi.org/10.1016/j.jhydrol.2022.127787

Gudmundsson, L., Boulange, J., Do, H. X., Gosling, S. N., Grillakis, M. G., Koutroulis, A. G., et al. (2021). Globally observed trends in mean and extreme river flow attributed to climate change. *Science*, *371*(6534), 1159–1162. https://doi.org/10.1126/science.aba3996

Gustafsson, M., Rayner, D., & Chen, D. (2010). Extreme rainfall events in southern Sweden: Where does the moisture come from? *Tellus A: Dynamic Meteorology and Oceanography*, *62*, 605–616. https://doi.org/10.3402/tellusa.v62i5.15715

Hersbach, H., Bell, B., Berrisford, P., Hirahara, S., Horányi, A., Muñoz-Sabater, J., et al. (2020). The ERA5 global reanalysis [Dataset]. *Quarterly Journal of the Royal Meteorological Society*, *146*(730), 1999–2049. https://doi.org/10.1002/qj.3803

Higgins, M. E., & Cassano, J. J. (2009). Impacts of reduced sea ice on winter Arctic atmospheric circulation, precipitation, and temperature. *Journal of Geophysical Research*, *114*(D16), D16107. https://doi.org/10.1029/2009jd011884

Hu, P., Chen, W., Huang, R., & Nath, D. (2018). On the weakening relationship between the South China Sea summer monsoon onset and cross-equatorial flow after the late 1990s. *International Journal of Climatology*, *38*(7), 3202–3208. https://doi.org/10.1002/joc.5472

Irannezhad, M., Liu, J., & Chen, D. (2021). Extreme precipitation variability across the Lancang-Mekong River Basin during 1952–2015 in relation to teleconnections and summer monsoons. *International Journal of Climatology*, *42*(5), 2614–2638. https://doi.org/10.1002/joc.7370

Jin, Q., & Wang, C. (2017). A revival of Indian summer monsoon rainfall since 2002. *Nature Climate Change*, *7*(8), 587–594. https://doi.org/10.1038/nclimate3348

Kalnay, E., Kanamitsu, M., Kistler, R., Collins, W., Deaven, D., Gandin, L., et al. (1996). The NCEP/NCAR 40-year reanalysis project [Dataset]. *Bulletin of the American Meteorological Society*, *77*(3), 437–472. https://doi.org/10.1175/1520-0477(1996)077<0437:tnyrp>2.0.co;2

Kohonen, T. (1990). The self-organizing map. *Proceedings of the IEEE*, *78*(9), 1464–1480. https://doi.org/10.1109/5.58325

Lemus-Canovas, M. (2022). Changes in compound monthly precipitation and temperature extremes and their relationship with teleconnection patterns in the Mediterranean. *Journal of Hydrology*, *608*, 127580. https://doi.org/10.1016/j.jhydrol.2022.127580

Li, C., Zwiers, F., Zhang, X., Chen, G., Lu, J., Li, G., et al. (2019). Larger increases in more extreme local precipitation events as climate warms. *Geophysical Research Letters*, *46*(12), 6885–6891. https://doi.org/10.1029/2019gl082908

Li, J., Zhao, Y., Chen, D., Kang, Y., & Wang, H. (2021). Future precipitation changes in three key sub-regions of east Asia: The roles of thermodynamics and dynamics. *Climate Dynamics*, *59*(5–6), 1377–1398. https://doi.org/10.1007/s00382-021-06043-w

Li, X., Long, D., Scanlon, B. R., Mann, M. E., Li, X., Tian, F., et al. (2022). Climate change threatens terrestrial water storage over the Tibetan Plateau. *Nature Climate Change*, *12*(9), 801–807. https://doi.org/10.1038/s41558-022-01443-0

Liu, B., Tan, X., Gan, T. Y., Chen, X., Lin, K., Lu, M., & Liu, Z. (2020). Global atmospheric moisture transport associated with precipitation extremes: Mechanisms and climate change impacts. *WIREs Water*, *7*(2), e1412. https://doi.org/10.1002/wat2.1412

Liu, K. S., & Chan, J. C. L. (2022). Growing threat of rapidly-intensifying tropical cyclones in east Asia. *Advances in Atmospheric Sciences*, *39*(2), 222–234. https://doi.org/10.1007/s00376-021-1126-7

Ma, Q., Hu, R., Wu, Y., Zhang, J., Zhi, R., & Feng, G. (2022). Variations in July extreme precipitation in Henan Province and the related mechanisms. *International Journal of Climatology*, *42*(16), 9115–9130. https://doi.org/10.1002/joc.7805

Muller, C., & Takayabu, Y. (2020). Response of precipitation extremes to warming: What have we learned from theory and idealized cloud-resolving simulations, and what remains to be learned? *Environmental Research Letters*, *15*(3), 035001. https://doi.org/10.1088/1748-9326/ab7130

Nanditha, J. S., Kushwaha, A. P., Singh, R., Malik, I., Solanki, H., Chuphal, D. S., et al. (2023). The Pakistan flood of August 2022: Causes and implications. *Earth's Future*, *11*(3). https://doi.org/10.1029/2022ef003230

Nie, Y., & Sun, J. (2022). Moisture sources and transport for extreme precipitation over Henan in july 2021. *Geophysical Research Letters*, *49*(4), e2021GL097446. https://doi.org/10.1029/2021gl097446

Nogueira, M. (2020). Inter-comparison of ERA-5, ERA-interim and GPCP rainfall over the last 40 years: Process-based analysis of systematic and random differences. *Journal of Hydrology*, *583*, 124632. https://doi.org/10.1016/j.jhydrol.2020.124632

Ramanathan, V., Chung, C., Kim, D., Bettge, T., Buja, L., Kiehl, J. T., et al. (2005). Atmospheric brown clouds: Impacts on South Asian climate and hydrological cycle. *Proceedings of the National Academy of Sciences of the United States of America*, *102*(15), 5326–5333. https://doi.org/10.1073/pnas.0500656102

Ratna, S. B., Cherchi, A., Osborn, T. J., Joshi, M., & Uppara, U. (2021). The extreme positive Indian Ocean Dipole of 2019 and associated Indian summer monsoon rainfall response. *Geophysical Research Letters*, *48*(2), 1–11. https://doi.org/10.1029/2020gl091497

Schewe, J., & Levermann, A. (2012). A statistically predictive model for future monsoon failure in India. *Environmental Research Letters*, *7*(4), 044023. https://doi.org/10.1088/1748-9326/7/4/044023

Shaw, R., Luo, Y., Cheong, T. S., Abdul Halim, S., Chaturvedi, S., Hashizume, M., et al. (2022). Asia. In *Climate change 2022: Impacts, adaptation, and vulnerability. Contribution of working group II to the sixth assessment report of the intergovernmental panel on climate change* (pp. 1457–1579).

Singh, D., Ghosh, S., Roxy, M. K., & McDermid, S. (2019). Indian summer monsoon: Extreme events, historical changes, and role of anthropogenic forcings. *WIREs Climate Change*, *10*(2), e571. https://doi.org/10.1002/wcc.571

Sinha, A., Kathayat, G., Cheng, H., Breitenbach, S. F. M., Berkelhammer, M., Mudelsee, M., et al. (2015). Trends and oscillations in the Indian summer monsoon rainfall over the last two millennia. *Nature Communications*, *6*(1), 6309. https://doi.org/10.1038/ncomms7309

Smith, A., Bates, P. D., Wing, O., Sampson, C., Quinn, N., & Neal, J. (2019). New estimates of flood exposure in developing countries using high-resolution population data. *Nature Communications*, *10*(1), 1814. https://doi.org/10.1038/s41467-019-09282-y

Stein, A. F., Draxler, R. R., Rolph, G. D., Stunder, B. J. B., Cohen, M. D., & Ngan, F. (2015). NOAA's HYSPLIT atmospheric transport and dispersion modeling system. *Bulletin of the American Meteorological Society*, *96*(12), 2059–2077. https://doi.org/10.1175/bams-d-14-00110.1

Sun, C., Xiao, Z.-N., & Nguyen, M. (2021). Projection on precipitation frequency of different intensities and precipitation amount in the Lancang-Mekong River basin in the 21st century. *Advances in Climate Change Research*, *12*(2), 162–171. https://doi.org/10.1016/j.accre.2021.03.001

Swain, D. L., Wing, O. E. J., Bates, P. D., Done, J. M., Johnson, K. A., & Cameron, D. R. (2020). Increased flood exposure due to climate change and population growth in the United States. *Earth's Future*, *8*(11), e2020EF001778. https://doi.org/10.1029/2020ef001778

Takahashi, H. G., & Yasunari, T. (2008). Decreasing trend in rainfall over indochina during the late summer monsoon: Impact of tropical cyclones. *Journal of the Meteorological Society of Japanese Series II*, *86*(3), 429–438. https://doi.org/10.2151/jmsj.86.429

Tan, X., Gan, T. Y., Chen, S., & Liu, B. (2018). Modeling distributional changes in winter precipitation of Canada using Bayesian spatiotemporal quantile regression subjected to different teleconnections. *Climate Dynamics*, *52*(3–4), 2105–2124. https://doi.org/10.1007/s00382-018-4241-0

Tan, X., Gan, T. Y., & Chen, Y. D. (2018). Synoptic moisture pathways associated with mean and extreme precipitation over Canada for summer and fall. *Climate Dynamics*, *52*(5–6), 2959–2979. https://doi.org/10.1007/s00382-018-4300-6

Tran, T. L., Ritchie, E. A., & Perkins-Kirkpatrick, S. E. (2022). A 50-year tropical cyclone exposure climatology in southeast Asia. *Journal of Geophysical Research: Atmospheres*, *127*(4), e2021JD036301. https://doi.org/10.1029/2021jd036301

Trenberth, K. E. (1998). Atmospheric moisture residence times and cycling: Implications for rainfall rates and climate change. *Climatic Change*, *39*(4), 667–694. https://doi.org/10.1023/a:1005319109110

Wang, C., & Wang, B. (2019). Tropical cyclone predictability shaped by western pacific subtropical high: Integration of trans-basin sea surface temperature effects. *Climate Dynamics*, *53*(5–6), 2697–2714. https://doi.org/10.1007/s00382-019-04651-1

Wang, S., Zhang, L., She, D., Wang, G., & Zhang, Q. (2021). Future projections of flooding characteristics in the Lancang-Mekong River Basin under climate change. *Journal of Hydrology*, *602*, 126778. https://doi.org/10.1016/j.jhydrol.2021.126778

Wang, Y., Long, D., & Li, X. (2023). High-temporal-resolution monitoring of reservoir water storage of the Lancang-Mekong River. *Remote Sensing of Environment*, *292*, 113575. https://doi.org/10.1016/j.rse.2023.113575

Wehrens, R., & Buydens, L. M. C. (2007). Self- and super-organizing maps inR: ThekohonenPackage [Software]. *Journal of Statistical Software*, *21*(5), 1–19. https://doi.org/10.18637/jss.v021.i05

Wehrens, R., & Kruisselbrink, J. (2018). Flexible self-organizing maps in kohonen 3.0 [Software]. *Journal of Statistical Software*, *87*(7), 1–18. https://doi.org/10.18637/jss.v087.i07

Wilson, S. S., Joseph, P. V., Mohanakumar, K., & Johannessen, O. M. (2018). Interannual and long term variability of low level jetstream of the Asian summer monsoon. *Tellus A: Dynamic Meteorology and Oceanography*, *70*(1), 1445380. https://doi.org/10.1080/16000870.2018.1445380

Xu, X., Dong, L., Zhao, Y., & Wang, Y. (2019). Effect of the Asian water tower over the Qinghai-Tibet plateau and the characteristics of atmospheric water circulation. *Chinese Science Bulletin*, *64*(27), 2830–2841. https://doi.org/10.1360/tb-2019-0203

Xu, X., Tian, H., Qie, K., He, X., Zhang, R., & Tu, H. (2020). A study on the trend of the upper tropospheric water vapor over the Tibetan plateau in summer. *Asia-Pacific Journal of Atmospheric Sciences*, *57*(2), 277–288. https://doi.org/10.1007/s13143-020-00191-5

Yamaguchi, M., Chan, J. C. L., Moon, I.-J., Yoshida, K., & Mizuta, R. (2020). Global warming changes tropical cyclone translation speed. *Nature Communications*, *11*(1), 47. https://doi.org/10.1038/s41467-019-13902-y

Yang, K., He, J., Tang, W., Qin, J., & Cheng, C. C. K. (2010). On downward shortwave and longwave radiations over high altitude regions: Observation and modeling in the Tibetan Plateau. *Agricultural and Forest Meteorology*, *150*(1), 38–46. https://doi.org/10.1016/j.agrformet.2009.08.004

Yang, R., Zhang, W.-K., Gui, S., Tao, Y., & Cao, J. (2019). Rainy season precipitation variation in the Mekong River basin and its relationship to the Indian and East Asian summer monsoons. *Climate Dynamics*, *52*(9–10), 5691–5708. https://doi.org/10.1007/s00382-018-4471-1

Yatagai, A., & Zhao, T. (2014). APHRODITE daily precipitation and temperature dataset: Development, QC, Homogenization and Spatial Correlation (p. 15588).

Yu, L., Zhong, S., Zhou, M., Lenschow, D. H., & Sun, B. (2018). Revisiting the linkages between the variability of atmospheric circulations and Arctic melt-season sea ice cover at multiple time scales. *Journal of Climate*, *32*(5), 1461–1482. https://doi.org/10.1175/jcli-d-18-0301.1

Zhang, C., Tang, Q., Chen, D., Ent, R., Liu, X., Li, W., & Haile, G. (2019). Moisture source changes contributed to different precipitation changes over the northern and southern Tibetan plateau. *Journal of Hydrometeorology*, *20*(2), 217–229. https://doi.org/10.1175/jhm-d-18-0094.1

Zhang, S., Chen, Y., Luo, Y., Liu, B., Ren, G., Zhou, T., et al. (2022). Revealing the circulation pattern most conducive to precipitation extremes in henan Province of north China. *Geophysical Research Letters*, *49*(7), e2022GL098034. https://doi.org/10.1029/2022gl098034

Zhao, J., Gan, T. Y., Zhang, G., & Zhang, S. (2023). Projected changes of precipitation extremes in North America using CMIP6 multi-climate model ensembles. *Journal of Hydrology*, *621*, 129598. https://doi.org/10.1016/j.jhydrol.2023.129598